Exact non-Hermitian mobility edges in one-dimensional quasicrystal lattice with exponentially decaying hopping and its dual lattice

Yanxia Liu [1,*] Yongjian Wang [2,3,*] Zuohuan Zheng,[2,3,4] and Shu Chen [1,5,6,†]

[1]*Beijing National Laboratory for Condensed Matter Physics, Institute of Physics, Chinese Academy of Sciences, Beijing 100190, China*
[2]*Academy of Mathematics and Systems Science, Chinese Academy of Sciences, Beijing 100190, China*
[3]*University of Chinese Academy of Sciences, Beijing 100049, China*
[4]*College of Mathematics and Statistics, Hainan Normal University Haikou, Hainan 571158, China*
[5]*School of Physical Sciences, University of Chinese Academy of Sciences, Beijing 100049, China*
[6]*Yangtze River Delta Physics Research Center, Liyang, Jiangsu 213300, China*

(Received 18 December 2020; accepted 14 April 2021; published 28 April 2021)

We analytically determine the non-Hermitian mobility edges of a one-dimensional quasiperiodic lattice model with exponentially decaying, hopping, and complex potentials as well as its dual model, which is just a non-Hermitian generalization of the Ganeshan-Pixley–Das Sarma model with nonreciprocal nearest-neighboring hopping. The presence of the non-Hermitian term destroys the self-duality symmetry and, thus, prevents us exploring the localization-delocalization point through looking for self-dual points. Nevertheless, by applying Avila's global theory, the Lyapunov exponent of the Ganeshan-Pixley–Das Sarma model can be exactly derived, which enables us to get an analytical expression of mobility edge of the non-Hermitian dual model. Consequently, the mobility edge of the original model is obtained by using the dual transformation, which creates exact mappings between the spectra and the wave functions of these two models.

DOI: 10.1103/PhysRevB.103.134208

I. INTRODUCTION

Anderson localization caused by disorder is an everlasting research topic in condensed-matter physics [1]. Although both random disorder [2–5] and quasiperiodic potential [6–10] can induce Anderson localization, a localization-delocalization transition is absent in low-dimensional random disorder systems. On the other hand, the localization-delocalization transition can occur even in one-dimensional (1D) quasiperiodic systems. In comparison with the random disorder systems, the quasiperiodic systems have their advantages for exploring some exact results due to the existence of duality relation for the transformation between real and momentum spaces. A simple but typical example is the Aubry-André (AA) model [8], which goes through a localization transition when the quasiperiodical potential strength exceeds a transition point, i.e., self-duality point. The study of various extensions of AA models reveals more diversified transition styles [10–15]. The quasiperiodic lattice models with short-range (long-range) hopping processes [16–22] or modified quasiperiodic potentials [23–25] can support energy-dependent mobility edges.

The combination of non-Hermiticity and disorder gives rise to many new perspectives for the localization phenomena. Due to throwing off the shackles of the Hermiticity constraint, non-Hermitian random matrices contain much more abundant symmetry classes according to Bernard-LeClair classification [26–29] than the corresponding Hermitian Altland-Zirnbauer classification. In the scheme of random matrix theory, non-Hermitian disorder systems behave differently in the spectral statistics in comparison with the Hermitian systems [30–33]. Recently, the interplay of the non-Hermitian effect and Anderson localization has attracted intensive studies in both random disorder systems [34–43] and quasiperiodic systems [44–56]. Although most previous works on non-Hermitian quasiperiodical systems focused on systems with only nearest-neighboring hopping, in this paper we study a 1D non-Hermitian quasicrystal lattice with long-range hopping and aim to give an analytical result for the mobility edges. Interplay of the long-range hopping and the quasiperiodic potential may generate some nontrivial localization properties [16,17,22]. The Hermitian limit of our model (1) can be reduced to the Biddle–Das Sarma model [16], which supports an analytical expression of mobility edges determined by a self-duality condition. However, the approach of searching the self-duality condition is failed for the non-Hermitian Biddle–Das Sarma model as the non-Hermitian term destroys the self-duality condition in the whole parameter spaces.

In order to explore the exact non-Hermitian mobility edges, we will take an alternative method and try to get an analytical expression of the Lyapunov exponent. The Lyapunov exponent is an important quantity to characterize the localization properties of disorder systems and was applied to obtain exact transition points for the non-Hermitian quasiperiodic models with nearest-neighbor hopping [54,56] by using Avila's global theory [57–60]. The key to this method is to determine the Lyapunov exponent. However, the analytical expression of the Lyapunov exponent for the system with long-range hopping is difficult to obtain, which prevents us

*These authors contributed equally to this work.
†schen@iphy.ac.cn

obtaining the exact mobility edges of model (1) directly. To make progress, we will study the dual model of the long-range hopping model, which is obtained by making a dual transformation to model (1). It is interesting to indicate that the dual model (4) is just a non-Hermitian generalization of the Ganeshan-Pixley–Das Sarma model [18] with nonreciprocal (or asymmetrical) nearest-neighboring hopping. The Ganeshan-Pixley–Das Sarma model also supports an analytical expression of mobility edges determined by a self-duality condition [18] and is actually a dual model of the Biddle–Das Sarma model [61]. The Lyapunov exponent of the Ganeshan-Pixley–Das Sarma model can be obtained by applying Avila's global theory [62], which allows us to obtain an analytical formula of the mobility edge of the dual model (4). The mobility edge not only splits the extended and localized states, but also splits the real and complex eigenvalues. Since the dual transformation converts model (1) and its dual model (4) each other and constructs exact mapping between their eigenvalues and the eigenstates, the mobility edge of the model with long-range hopping can be obtained by the substitution of parameters from the analytical expression of mobility edge of the dual model.

II. MODELS AND RESULTS

We consider a 1D quasiperiodic model with long-range hopping terms and a complex potential, described by

$$E\phi_n = \sum_{n'\neq n} t e^{-p|n-n'|}\phi_{n'} + V\ \cos(2\pi\omega n + ih)\phi_n, \qquad (1)$$

where $p > 0$ represents the decay rate, $V \in \mathbb{R}$ is the quasiperiodic potential strength, ω is an irrational number, and h describes a complex phase factor. We set $t = 1$ as the unit of energy and choose $\omega = (\sqrt{5}-1)/2$. We note that the system described by Eq. (1) possesses parity-time ($\mathcal{PT}$) symmetry [63] with the corresponding Hamiltonian,

$$H = \sum_{n'\neq n} t e^{-p|n-n'|}|n'\rangle\langle n| + \sum_n V\ \cos(2\pi\omega n + ih)|n\rangle\langle n|, \qquad (2)$$

keeping unchanged under parity operation $n \to -n$ and time-reversal operation by taking complex conjugation. When $h = 0$, i.e., the Hermitian case, the model has been studied in Refs. [16,17] and an analytical expression of the mobility edge is obtained by applying a self-dual transformation. For the non-Hermitian case with $h \neq 0$, no self-duality relation exists, and no analytical result is known. In a recent work [51], it has been shown that there exists a mobility edge which can be well fitted by the expression of $E = Ve^{|h|}\cosh(p) - 1$ when both h and $p \gg 1$. However, numerical results unveil that the above conjectured expression fails to describe the mobility edge in the region with small h and p.

In this paper, we analytically derive the exact mobility edge for model (1) with arbitrary p and h. The mobility edge segregating the localized and extended states can be represented as an extremely simple expression,

$$E = V\ \cosh(p + |h|) - 1 \qquad (3)$$

for the eigenvalues. In general, the eigenvalues of non-Hermitian systems are complex. The above expression indicates that the mobility edge is real, and, thus, the mobility edge also separates the real and complex states.

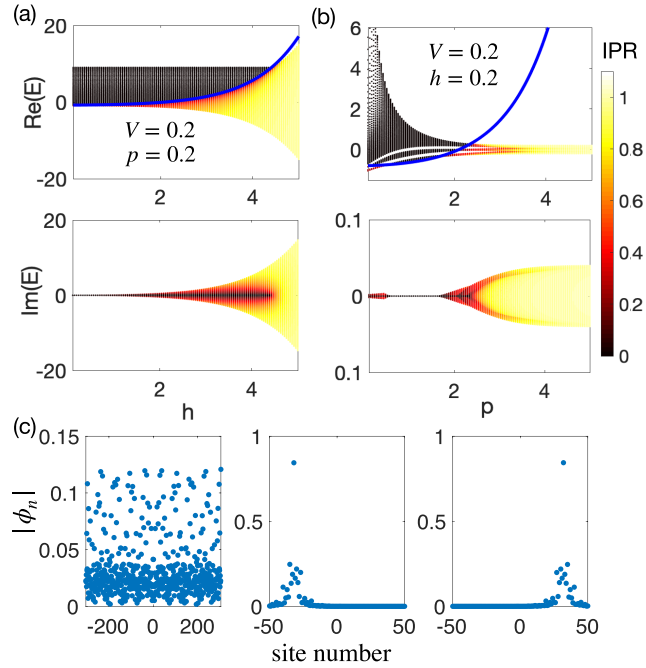

FIG. 1. (a) The real and imaginary parts of the eigenvalue spectra versus h for the system under the periodic boundary condition with $V = 0.2$, $p = 0.2$, and $N = 610$. (b) The real and imaginary parts of the eigenvalue spectra versus p for the system under the periodic boundary condition with $V = 0.2$, $h = 0.2$, and $N = 610$. (c) Distributions of eigenstates corresponding to different eigenvalues for the system with $p = 0.2$, $V = 0.2$, and $h = 2.5$. The eigenvalues are, from left to right: $E = 0.95$, $-0.69 + 0.94i$, and $-0.69 - 0.94i$, respectively.

Before deriving Eq. (3), we first show the consistency of analytical and numerical results and give numerical verification of the mobility edge. In order to characterize the localization-delocalization transition of a wave function, we numerically calculate the inverse partition ratio (IPR) of an eigenstate, which is defined as $\mathrm{IPR}^{(i)} = (\sum_n |\phi_n^i|^4)/(\sum_n |\phi_n^i|^2)^2$ where the superscript i labels the ith eigenstate of system and n represents the coordinate of the lattice site. Although $\mathrm{IPR} \simeq 1/L$ approaches zero for an extended eigenstate when the lattice size $L \to \infty$, $\mathrm{IPR} \simeq 1$ for a fully localized eigenstate.

In Fig. 1(a), we plot the IPR of different eigenstates versus the complex phase factor h for the system with $V = 0.2$ and $p = 0.2$. The eigenstates are characterized by their real and imaginary parts of the corresponding eigenvalues, respectively. The blue solid line represents the transition points determined by Eq. (3), which separates the extended and localized states. It is shown that the analytical relation of the mobility edge agrees well with numerical results from IPR and spectrum calculations. With the increase in complex phase factor h, the effective complex potential strength increases, and it causes more eigenstates to become localized. Consequently, the system undergoes the extended, intermediate, and localized regime when h increases. In Fig. 1(b), we plot the real parts and imaginary parts of eigenvalues as well as the

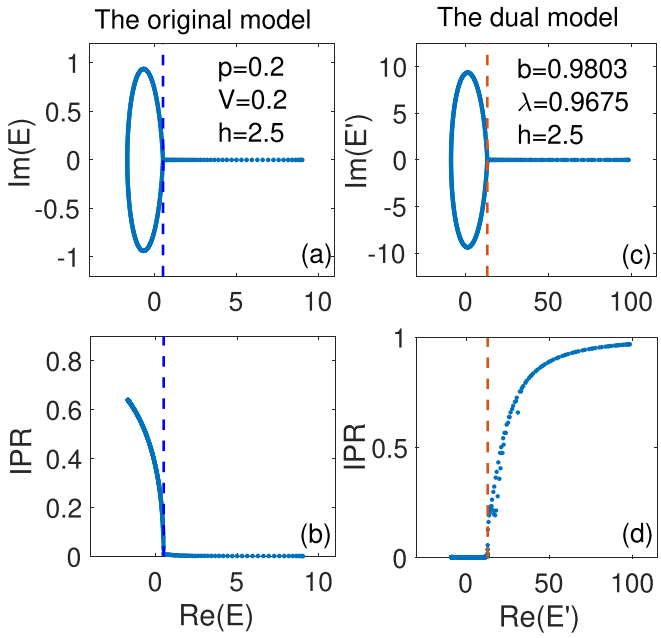

FIG. 2. (a) The energy spectrum and (b) the IPR of eigenstates for model (1) under the periodic boundary condition with $h = 2.5$, $V = 0.2$, $p = 0.2$, and $N = 610$. The blue dashed lines represent the exact mobility edges (3). (c) The energy spectrum and (d) the IPR of eigenstates for the dual model (4) under the periodic boundary condition with $h = 2.5$, $\lambda = 0.9675$, $b = 0.9803$, and $N = 610$. The orange dashed lines represent the exact mobility edges (18).

IPR of the corresponding wave functions versus the decay rate p by fixing $V = 0.2$ and $h = 0.2$. The blue solid line marks the transition points determined by Eq. (3), which agree well with numerical results. When $p > 2.35$, all eigenvalues are complex and below the blue curve. For both cases displayed in Figs. 1(a) and 1(b), eigenstates above the blue curves have real eigenvalues and keep $\mathcal{PT}$ symmetry, whereas eigenstates below the blue curves have complex-conjugated eigenvalues and, thus, are $\mathcal{PT}$-symmetry broken. So the mobility edge also separates the $\mathcal{PT}$-symmetry region from the $\mathcal{PT}$-symmetry-broken region.

To get a straightforward understanding, we display the distributions of eigenstates corresponding to different eigenvalues for the system with $p = 0.2$, $V = 0.2$, and $h = 2.5$ in Fig. 1(c). The corresponding spectrum of the system is displayed in Fig. 2(a) with the mobility edges $E_c = 0.5$ according to Eq. (3). It is clear that the eigenstate with real eigenvalue $E = 0.95$ above E_c is an extended state, which preserves the PT symmetry. On the other hand, the eigenstates with complex eigenvalues $E = -0.69 \pm 0.94i$ are localized states, which break the PT symmetry.

It is quite interesting to indicate that part of the eigenstates becomes localized in the region of a small p, As $p \to 0$, the hopping amplitude between long-range sites decays slowly, and long-range hopping terms will play an important role. Intuitively, this is counterintuitive because the long-range hopping generally tends to delocalize the localized states. To understand why this happens, we consider the limit case with $p = 0$ and $V = 0$ in which the model with equal hopping terms has a $(N-1)$-degenerate eigenstates. When a finite V is introduced, $(N-1)$-degenerate eigenstates all become the localized states. A small p lifts the degeneracy and tends to turn the localized states into the extended states. On the other hand, in the large-p limit the hopping amplitude between long-range sites decays very quickly, and the system with a large p can be viewed as a short-range hopping model with the nearest-neighbor hopping amplitude $t_1 = te^{-p}$ playing a dominate role. If we omitted all the long-range terms, the system can be approximately described by the AA model, and, thus, all the eigenstates of system become localized as long as $V > 2t_1$.

Now we return back to discuss how to derive Eq. (3). Instead of directly solving the original model of Eq. (1), we will derive the analytical expression of mobility edge by solving its dual model, i.e., a nearest-neighbor nonreciprocal hopping non-Hermitian model described by

$$E'u_j = e^{-h}u_{j+1} + e^{h}u_{j-1} + V_j u_j, \tag{4}$$

with

$$V_j = 2\lambda \frac{\cos(2\pi\omega j)}{1 - b\cos(2\pi\omega j)}, \tag{5}$$

where

$$b = S(p) = \frac{1}{\cosh(p)}, \tag{6}$$

$$\lambda = \frac{S(p)[1 - e^{-p}S(p)]}{V}, \tag{7}$$

and

$$E' = \frac{2[E + e^{-p}S(p)]}{V}. \tag{8}$$

The model described by Eq. (4) can be obtained from model of Eq. (1) through the following transformation:

$$\phi_n = \sum_n e^{i2\pi\omega n j} u_j. \tag{9}$$

Models (4) and (1) are dual models with parameters connected by Eqs. (6)–(8). The complex phase factor h in model (1) becomes the imaginary vector potential in model (4). The corresponding Hamiltonian for model (4) is given by

$$H = \sum_j (e^{-h}|j\rangle\langle j+1| + e^{h}|j+1\rangle\langle j| + V_j|j\rangle\langle j|). \tag{10}$$

Model (4) can be viewed as a generalization of the Hatano-Nelson model [34,35] with the on-site random potential replaced by the quasiperiodic potential V_j. The impact of the imaginary vector potential on the Anderson localization has been studied in terms of the Hatano-Nelson model. In comparison with the the Hatano-Nelson model, our generalized model (4) can give an analytical result for the mobility edges.

Now we analytically derive the mobility edge of model (4). First we consider the case of $h = 0$ and calculate the Lyapunov exponent of the system. The Lyapunov exponent can be evaluated based on the transfer matrix, which can be represented as

$$\gamma(E') = \lim_{n\to\infty} \frac{1}{2\pi n} \int \ln \|T_n(E', \phi)\| d\phi, \tag{11}$$

where $\| T_n \|$ denotes the norm of the transfer matrix given by

$$T_n(E', \phi) = \prod_{j=1}^{n} M_j = \prod_{j=1}^{n} \begin{pmatrix} E' - V_j & -1 \\ 1 & 0 \end{pmatrix}.$$

From the discussions in Refs. [54,60], we know that if the energy E' lies in the spectrum of the Hamiltonian H, we have

$$\gamma(E') = \max\{\gamma_c(E'), 0\}, \tag{12}$$

where $\gamma_c(E')$ is analytically given by

$$\gamma_c(E') = \ln \left| \frac{|bE' + 2\lambda| + \sqrt{(bE' + 2\lambda)^2 - 4b^2}}{2(1 + \sqrt{1 - b^2})} \right|. \tag{13}$$

The details for the derivation of the above analytical expression can be found in Appendix A. Although $\gamma(E') > 0$ corresponds to the localized state, the extended state is characterized by $\gamma(E') = 0$. Therefore, the mobility edge can be determined by $\gamma_c(E') = 0$ and operator theory, which gives rise to

$$E' = 2\,\mathrm{sgn}(\lambda)\frac{(1 - |\lambda|)}{b}. \tag{14}$$

The details for the analysis of the above result can be found in Appendix B. The mobility edge of model (4) with $h = 0$ can also be obtained by looking for the self-dual points of system, which was originally given in Ref. [18]. Our method based on the analytical expression of the Lyapunov exponent results in the same result. Although Eq. (14) is known, we note that the analytical expression of the Lyapunov exponent was only derived recently [62].

For the general case with $h \neq 0$, the system does not have a self-duality point in the parameter space. A nonzero h induces the nonreciprocal hopping, which breaks the Hermiticity of the system and may cause skin effect for the system under open boundary condition. A similar transformation can transform the non-Hermitian Hamiltonian $H(h)$ under the open boundary condition into a Hermitian Hamiltonian H', via

$$H' = SH(h)S^{-1}, \tag{15}$$

where

$$S = \mathrm{diag}(e^{-h}, e^{-2h}, \ldots, e^{-Nh})$$

is a similarity matrix with only diagonal entries and $H' = H(h = 0)$ is the Hermitian Hamiltonian with $h = 0$. The relation between the eigenstates of H and H' is achieved naturally: $|\psi\rangle = S^{-1}|\psi'\rangle$. Here $|\psi\rangle = \sum_j u_j|j\rangle$ is the eigenstate of H, and $H|\psi\rangle = E'|\psi\rangle$ gives rise to Eq. (4). The transformation S^{-1} can convert the extended states $|\psi'\rangle$ into skin states, which exponentially gather the wave function all to one of boundaries [34,35,47,64–68].

A localized state of H' may be expressed in a unified compact form

$$|u_i| \propto e^{-|i-i_0|/\xi},$$

where i_0 represents the position of localization center of a given localized state, $\xi = 1/\gamma$ is the localization length, and γ is the Lyapunov exponent of the localized state for the system of $h = 0$. Then the corresponding wave function of $H(h)$ takes the following form:

$$|u_i| \propto e^{hi - \gamma|i-i_0|}, \tag{16}$$

which exhibits different decaying behaviors on different sides of the localization center. When $|h| \geqslant \gamma$, delocalization occurs on one side [34,35,47], and, thus, the transition point from the localized state to the skin state is given by

$$\gamma = |h|. \tag{17}$$

Since a localized state apart from boundaries is not affected by the boundary condition of the system, it then follows that the boundary of localization-delocalization transition under the periodic boundary condition is also given by Eq. (17). Bringing Eq. (12) into Eq. (17), we can get the mobility edges which can be expressed as

$$E'_c = \frac{2\,\mathrm{sgn}(\lambda)(\cosh|h| + \sqrt{1 - b^2}\sinh|h| - |\lambda|)}{b}. \tag{18}$$

Equation (18) with $h = 0$ can be reduced to Eq. (14). Replacing the parameters b, λ, and E' with p, V, and E, we can rewrite Eq. (18) as Eq. (3). Although the mobility edges of a model can be read out from its dual model, the eigenstates of a model and its dual model are distinct. If the eigenstates of a model are localized, the eigenstates of its dual model are extended, and vice versa.

In Figs. 2(a) and 2(b), we plot the energy spectrum and the numerical results of the IPR versus eigenenergies E for model (1) with $h = 2.5$, $V = 0.2$, $p = 0.2$, and $N = 610$. The eigenstates of model (1) with eigenenergies $\mathrm{Re}(E) < E_c$, where $E_c = V\ \cosh(p + |h|) - 1$ are localized states, and the corresponding IPRs of these states take finite values. On the other hand, the IPRs of states with $E > E_c$ approach zero, corresponding to extended states. The mobility edge E_c not only separates the localized and delocalized states, but also real and complex eigenenergies of the model. Figure 2(c) displays the energy spectrum of dual model (4) with the same parameters as in Fig. 2(a). The energy spectra displayed in Figs. 2(a) and 2(c) have similar structures and can be mapped to each other by using the linear relation between E and E' given by Eq. (8). Figure 2(d) shows the numerical results of the IPR versus eigenenergies E'. Here the IPR for the ith eigenstate of the dual model is defined as $\mathrm{IPR}^{(i)} = (\sum_n |u_n^i|^4)/(\sum_n |u_n^i|^2)^2$. The eigenergeis of extended states for model (4) lie in $\mathrm{Re}(E') < E'_c$, whereas the localized states distribute in $E' > E'_c$.

In Fig. 3(a1), we plot the real and imaginary parts of eigenvalues as well as the IPR of the corresponding wave functions versus the potential strength V by fixing $h = 0.5$ and $p = 1$ for original model (1). The results of dual model (4) with corresponding parameters $h = 0.5$ and $b = 0.648$ are shown in Fig. 3(b1), where E' and λ can be mapped to E and V via Eqs. (8) and (7), respectively. The blue solid lines in Figs. 3(a1) and 3(b1) mark the transition points determined by Eqs. (3) and (18), respectively. We plot spectrum structure on the complex plane with various V's and their corresponding λ in Figs. 3(a2) and 3(b2), which clearly show the existence of dual relations between these two models.

We note that model (1) has $\mathcal{PT}$ symmetry [51,63] and there exists a $\mathcal{PT}$-symmetry unbroken region with all eigenvalues

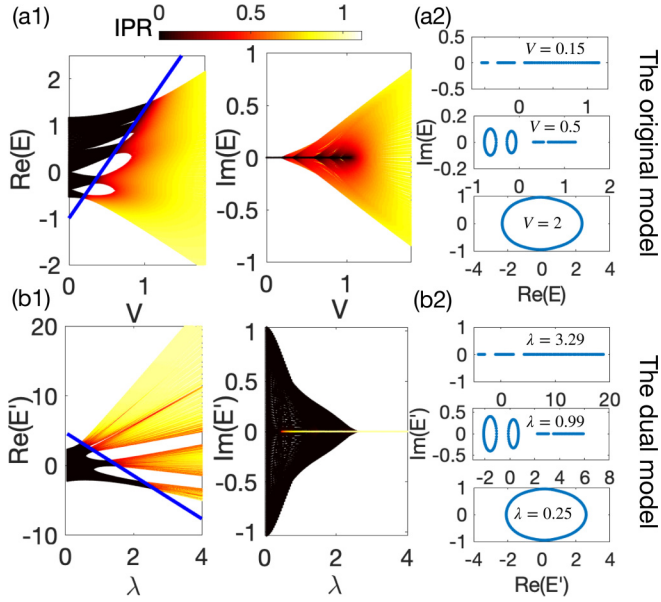

FIG. 3. (a1) The real and the imaginary parts of the eigenvalue spectra of the original model (1) versus V for the system with $p = 1$, $h = 0.5$, and $N = 233$. (a2) The energy spectrum of eigenstates with $V = 0.15,\ 0.5$, and 2, respectively. (b1) The real and the imaginary parts of the eigenvalue spectra of the dual model (4) versus λ for the system with $b = 0.648$, $h = 0.5$, and $N = 233$. (b2) The energy spectrum of eigenstates with $\lambda = 3.29,\ 0.99$, and 0.25, respectively. The blue solid lines represent the exact mobility edges (3) or (18). Here we have taken the periodic boundary condition.

being real when $V < V_c$. For model (4), there exists a region with all eigenvalues being real for $\lambda > \lambda_c$. With the help of the dual relation, we can give an explanation why there exists a localized region with real eigenvalues for model (4). Although model (4) has no obvious $\mathcal{PT}$ symmetry, its dual model (1) has $\mathcal{PT}$ symmetry, and the extended states correspond to the real eigenvalues. It has been demonstrated that the localization transition induced by the non-Hermitian quasiperiodic potential always occurs at the $\mathcal{PT}$-symmetry-breaking point [51]. For the type of Hatano-Nelson models, it has been already explained why the eigenvalues of localized states have real spectra without the need to resort to the dual transformation [34,35,47,69].

The non-Hermitian quasiperiodic potentials may be implemented in photonic lattices [70–76]. Recently, a few representative non-Hermitian phenomena are observed on the photonic systems, such as $\mathcal{PT}$ symmetry, exceptional points, non-Hermitian skin effect., etc. [70–76]. The mobility edges may be experimentally realized in photonic systems.

III. SUMMARY

To summarize, we studied exact localization transition for the non-Hermitian model with the exponentially decaying hopping and complex potential, which lacks self-duality symmetry but can be mapped to a nonreciprocal Ganeshan-Pixley–Das Sarma model with only nearest-neighbor hopping. The exact Lyapunov exponent $\gamma(E)$ of the dual model with $h = 0$ can be obtained by applying Avila's global theory. In the presence of nonreciprocal hopping, the localization-delocalization transition occurs as long as $h = \gamma(E)$, which determines analytically the mobility edges of the dual model. By using the dual transformation, the analytical expression of mobility edges for the original model is obtained. The dual transformation also constructs exact mappings between the spectra and the wave functions of the original and dual models.

ACKNOWLEDGMENTS

This work was supported by the National Key Research and Development Program of China (Grant No. 2016YFA0300600), NSFC under Grant No. 11974413 and the Strategic Priority Research Program of CAS (Grant No. XDB33000000). Z.Z. acknowledges financial support from the NSF of China (Grants No. 12031020 and No. 11671382), the CAS Key Project of Frontier Sciences (Grant No. QYZDJ-SSW-JSC003), the Key Laboratory of Random Complex Structures and Data Sciences CAS, and the National Center for Mathematics and Interdisciplinary Sciences CAS. Y.W. was supported by the NSF of China (Grant No. 12061031).

APPENDIX A: THE DETAILS FOR THE LYAPUNOV EXPONENT

We use Avila's global theory to calculate the Lyapunov exponent (LE) of the following Schrödinger equation:

$$(Hu)_j = u_{j+1} + u_{j-1} + V_j u_j = E u_j, \qquad j \in \mathbb{Z}, \tag{A1}$$

where

$$V_j = 2\lambda \frac{\cos(2\pi\omega j + \phi)}{1 - b\cos(2\pi\omega j + \phi)}, \qquad b \in (-1, 1), \quad \lambda \neq 0, \tag{A2}$$

V_j is the potential, b is the parameter, ϕ is the phase, $\lambda \in \mathbb{R}$ is the coupling, and the frequency $\omega \in \mathbb{R}$ is irrational.

The Lyapunov exponent can be evaluated based on the transfer matrix technique. Model (A1) can be transformed into the form

$$\begin{pmatrix} u_{j+1} \\ u_j \end{pmatrix} = M_j \begin{pmatrix} u_j \\ u_{j-1} \end{pmatrix} = M_j M_{j-1} \cdots M_1 \begin{pmatrix} u_1 \\ u_0 \end{pmatrix}, \tag{A3}$$

where the transfer matrix M_j is given by

$$M_j = \begin{pmatrix} E - V_j & -1 \\ 1 & 0 \end{pmatrix}. \tag{A4}$$

The transfer matrix is

$$T_n(E, \phi) = M_n M_{n-1} \cdots M_1 = \prod_{j=1}^{n} M_j.$$

The Lyapunov exponent about $T_n(E, \phi)$ is defined as

$$\gamma(E) = \lim_{n\to\infty} \frac{1}{2\pi n} \int \ln \|T_n(\phi)\| d\phi.$$

It is obvious that $\gamma(E) \geqslant 0$ due to $\det T_n(E) = 1$.

The first stage in the calculation of the LE is the complex of the phase, i.e., $\phi \to \phi + i\epsilon$. The potential becomes

$$V_j(\phi + i\epsilon) = 2\lambda \frac{\cos(2\pi\omega j + \phi + i\epsilon)}{1 - b\cos(2\pi\omega j + \phi + i\epsilon)}.$$

We induce a new matrix $\widetilde{M}_j$, which can be written as

$$\begin{aligned}\widetilde{M}_j(\phi) &= [1 - b\cos(2\pi\omega j + \phi)]M_j \\ &= [1 - b\cos(2\pi\omega j + \phi)]\begin{pmatrix} E - V_j & -1 \\ 1 & 0 \end{pmatrix} \\ &= \begin{pmatrix} E - (bE + 2\lambda)\cos(2\pi\omega j + \phi) & -1 + b\cos(2\pi\omega j + \phi) \\ 1 - b\cos(2\pi\omega j + \phi) & 0 \end{pmatrix}, \end{aligned} \tag{A5}$$

due to the complexity of matrix M_j. The transfer matrix for $\widetilde{M}_j(\phi)$ can be expressed as

$$\widetilde{T}_n(E, \phi) = \prod_{j=1}^{n} \widetilde{M}_j(\phi).$$

The Lyapunov exponent about $\widetilde{T}_n(E, \phi + i\epsilon)$ is

$$\tilde{\gamma}(E, \phi + i\epsilon) = \lim_{n\to\infty} \frac{1}{2\pi n} \int \ln \|\widetilde{T}_n(E, \phi + i\epsilon)\| d\phi.$$

It is easy to see that

$$\begin{aligned}\gamma(E, \epsilon) &= \tilde{\gamma}(E, \epsilon) - \lim_{n\to\infty} \frac{1}{2\pi n} \sum_{j=1}^{n} \ln[1 - b\cos(2\pi\omega j + i\epsilon)] \\ &= \tilde{\gamma}(E, \epsilon) - \frac{1}{2\pi} \int_0^{2\pi} \ln[1 - b\cos(\phi + i\epsilon)] d\phi \\ &= \tilde{\gamma}(E, \epsilon) - \ln \frac{1 + \sqrt{1 - b^2}}{2}, \\ &\quad \text{if } |\epsilon| < \ln \left| \frac{1 + \sqrt{1 - b^2}}{b} \right|. \end{aligned} \tag{A6}$$

This means that $\gamma(E, \epsilon)$ and $\tilde{\gamma}(E, \epsilon)$ has the same slope about ϵ when $|\epsilon| < \ln|\frac{1+\sqrt{1-b^2}}{b}|$.

In the large-ϵ limit, we get

$$\widetilde{T}_n(E, \epsilon) = \frac{1}{2} e^{-2\pi\omega n i + |\epsilon|} \begin{pmatrix} -bE - 2\lambda & b \\ -b & 0 \end{pmatrix} + o(1). \tag{A7}$$

Avila's global theory can be extended to the general case and it shows that $\tilde{\gamma}(E, \epsilon)$ is a convex, piecewise linear function about $\epsilon \in (-\infty, \infty)$. For model (A1), in the large-ϵ limit, the slope about ϵ is always 1, which further implies that

$$\tilde{\gamma}(E, \epsilon) = |\epsilon| + \ln f(E),$$

for large enough ϵ, where

$$f(E) = \left| \frac{|bE + 2\lambda| + \sqrt{(bE + 2\lambda)^2 - 4b^2}}{4} \right|.$$

Moreover, by the convexity of $\tilde{\gamma}(E, \epsilon)$ about ϵ, we have

$$\tilde{\gamma}(E, \epsilon) \geqslant \ln f(E), \tag{A8}$$

thus,

$$\gamma(E, \epsilon) \geqslant \max\left\{ \ln \frac{2f(E)}{1 + \sqrt{1 - b^2}}, 0 \right\}. \tag{A9}$$

Here we make use of $\gamma(E, \epsilon) \geqslant 0$.

For the finite $0 \leqslant \epsilon < \ln|\frac{1+\sqrt{1-b^2}}{b}|$, by Avila's global theory, the slope of $\gamma(E, \epsilon)$ might be 1 or 0, since Lyapunov eponent $\gamma(E, \epsilon)$ is convex, moreover, the slope of $\gamma(E, \epsilon)$ in a neighborhood of $\epsilon = 0$ is nonzero if the energy E is in the spectrum and the Lyapunov exponent $\gamma(E, 0) > 0$. By equation (A6), when $|\epsilon| < \ln|\frac{1+\sqrt{1-b^2}}{b}|$, the slope of $\tilde{\gamma}(E, \epsilon)$ is equal to that of $\gamma(E, \epsilon)$. Thus, when $\gamma(E, 0) > 0$, $0 \leqslant \epsilon < \ln|\frac{1+\sqrt{1-b^2}}{b}|$ and E is in the spectrum, the slope of $\tilde{\gamma}(E, \epsilon)$ is also 1.

When $\gamma(E, 0) > 0$ since the Lyapunov exponent $\tilde{\gamma}(E, \epsilon)$ is convex and continuous, thus, the slope of $\tilde{\gamma}(E, \epsilon)$ is always 1, which implies that

$$\tilde{\gamma}(E, \epsilon) = |\epsilon| + \ln f(E), \tag{A10}$$

for any $\epsilon \in (-\infty, \infty)$. According to Eq. (A6) and the nonnegativity of Lyapunov exponent $\gamma(E, \epsilon)$, we have

$$\gamma(E, 0) = \max\left\{ \ln \frac{2f(E)}{1 + \sqrt{1 - b^2}}, 0 \right\}, \tag{A11}$$

if $\gamma(E, 0) > 0$ and E is in the spectrum.

When $\gamma(E, 0) = 0$, the right side of Eq. (A9) is 0. Thus, the energy E also satisfies Eq. (A11). Based on above discussion and analysis, we deduce

$$\gamma(E, 0) = \max\left\{ \ln \frac{2f(E)}{1 + \sqrt{1 - b^2}}, 0 \right\} \tag{A12}$$

for every E in the spectrum.

APPENDIX B: MOBILITY EDGES

The mobility edge can be roughly determined by $\gamma_c(E) = 0$, which gives

$$|bE + 2\lambda| = 2.$$

The more accurate mobility edge can be obtained by operator theory.

The operator theory tells us that the spectrum $\{E_j\}$ of model (A1) and V_j have the relation $\{E_j\} \subseteq [-2 + \min_j(V_j), 2 + \max_j(V_j)]$. Thus, when $\lambda > 0$, we have

$$\{E_j\} \subseteq \left[-2 - \frac{2\lambda}{1 + b}, 2 + \frac{2\lambda}{1 - b} \right], \tag{B1}$$

and when $\lambda < 0$, we have

$$\{E_j\} \subseteq \left[-2 + \frac{2\lambda}{1-b}, 2 - \frac{2\lambda}{1+b}\right]. \tag{B2}$$

The eigenenergies of localized states satisfy $\gamma(E) = \gamma(E, 0) > 0$, which can give us that

$$|bE + 2\lambda| > 2.$$

First, we consider the case $\lambda > 0$. Assume $bE + 2\lambda < -2$, i.e.,

$$\begin{aligned} E &< \frac{-2-2\lambda}{b}, \quad b > 0, \\ E &> \frac{-2-2\lambda}{b}, \quad b < 0. \end{aligned} \tag{B3}$$

From condition (B1), we can get

$$-2 - \frac{2\lambda}{1-b} \leqslant E \leqslant 2 + \frac{2\lambda}{1-b}.$$

Since

$$\frac{-2-2\lambda}{b} < -2 - \frac{2\lambda}{1+b},$$

with $b > 0$ and

$$\frac{-2-2\lambda}{b} > 2 + \frac{2\lambda}{1-b},$$

with $b < 0$, this leads to contradictions. When $\lambda > 0$, the eigenenergies of localized states only satisfy $bE + 2\lambda > 2$.

Second, we consider the case of $\lambda < 0$. Assume $bE + 2\lambda > 2$, i.e.,

$$\begin{aligned} E &> \frac{2-2\lambda}{b}, \quad b > 0, \\ E &< \frac{2-2\lambda}{b}, \quad b < 0. \end{aligned} \tag{B4}$$

From condition (B2), we can get

$$-2 + \frac{2\lambda}{1-b} \leqslant E \leqslant 2 - \frac{2\lambda}{1-b}.$$

Since

$$\frac{2-2\lambda}{b} > 2 - \frac{2\lambda}{1+b},$$

with $b > 0$, and

$$\frac{2-2\lambda}{b} < -2 + \frac{2\lambda}{1-b},$$

with $b < 0$, this leads to contradictions. When $\lambda < 0$, the eigenenergies of localized states only satisfy $bE + 2\lambda < -2$.

In conclusion, for the eigenenergies of localized states, the Lyapunov exponent $\gamma(E) > 0$ if and only if

$$\begin{aligned} bE &> 2\,\mathrm{sgn}(\lambda)(1 - |\lambda|), \quad \lambda > 0, \\ bE &< 2\,\mathrm{sgn}(\lambda)(1 - |\lambda|), \quad \lambda < 0, \end{aligned}$$

it is equal to

$$\mathrm{sgn}(\lambda) bE > 2(1 - |\lambda|).$$

Thus, for the eigenenergies of extended states with Lyapunov exponent $\gamma(E) = 0$, we can get

$$\mathrm{sgn}(\lambda) bE < 2(1 - |\lambda|).$$

The mobility edge is

$$bE = 2\,\mathrm{sgn}(\lambda)(1 - |\lambda|).$$

[1] P. W. Anderson, Absence of diffusion in certain random lattices, Phys. Rev. **109**, 1492 (1958).

[2] E. Abrahams, P. W. Anderson, D. C. Licciardello, and T. V. Ramakrishnan, Scaling Theory Of Localization: Absence Of Quantum Diffusion In Two Dimensions, Phys. Rev. Lett. **42**, 673 (1979).

[3] D. J. Thouless, A relation between the density of states and range of localization for one dimensional random systems, J. Phys. C: Solid State Phys. **5**, 77 (1972).

[4] P. A. Lee and T. V. Ramakrishnan, Disordered electronic systems, Rev. Mod. Phys. **57**, 287 (1985).

[5] F. Evers and A. D. Mirlin, Anderson transitions, Rev. Mod. Phys. **80**, 1355 (2008).

[6] G. Roati, C. DErrico, L. Fallani, M. Fattori, C. Fort, M. Zaccanti, G. Modugno, M. Modugno, and M. Inguscio, Anderson localization of a non-interacting bose Ceinstein condensate, Nature (London) **453**, 895 (2008).

[7] H. P. Lüschen, S. Scherg, T. Kohlert, M. Schreiber, P. Bordia, X. Li, S. Das Sarma, and I. Bloch, Single-Particle Mobility Edge In A One-Dimensional Quasiperiodic Optical Lattice, Phys. Rev. Lett. **120**, 160404 (2018).

[8] S. Aubry and G. André, Analyticity breaking and Anderson localization in incommensurate lattices, Ann. Israel Phys. Soc. **3**, 133 (1980).

[9] D. J. Thouless, Localization By A Potential With Slowly Varying Period, Phys. Rev. Lett. **61**, 2141 (1988).

[10] M. Kohmoto, Metal-Insulator Transition And Scaling For Incommensurate Systems, Phys. Rev. Lett. **51**, 1198 (1983).

[11] L. Zhou, H. Pu, and W. Zhang, Anderson localization of cold atomic gases with effective spin-orbit interaction in a quasiperiodic optical lattice, Phys. Rev. A **87**, 023625 (2013).

[12] M. Kohmoto and D. Tobe, Localization problem in a quasiperiodic system with spin-orbit interaction, Phys. Rev. B **77**, 134204 (2008).

[13] X. Cai, L.-J. Lang, S. Chen, and Y. Wang, Topological Superconductor To Anderson Localization Transition In One-Dimensional Incommensurate Lattices, Phys. Rev. Lett. **110**, 176403 (2013).

[14] W. DeGottardi, D. Sen, and S. Vishveshwara, Majorana Fermions In Superconducting 1D Systems Having Periodic, Quasiperiodic, And Disordered Potentials, Phys. Rev. Lett. **110**, 146404 (2013).

[15] Y.-C. Wang, X.-J. Liu, and S. Chen, Properties and applications of one dimensional quasiperiodic lattices, Acta Phys. Sin. **68**, 040301 (2019).

[16] J. Biddle and S. Das Sarma, Predicted Mobility Edges In One-Dimensional Incommensurate Optical Lattices: An Exactly Solvable Model Of Anderson Localization, Phys. Rev. Lett. **104**, 070601 (2010).

[17] J. Biddle, D. J. Priour, B. Wang, and S. Das Sarma, Localization in one-dimensional lattices with non-nearest-neighbor hopping: Generalized Anderson and Aubry- André models, Phys. Rev. B **83**, 075105 (2011).

[18] S. Ganeshan, J. H. Pixley, and S. Das Sarma, Nearest Neighbor Tight Binding Models With An Exact Mobility Edge In One Dimension, Phys. Rev. Lett. **114**, 146601 (2015).

[19] X. P. Li, J. H. Pixley, D. L. Deng, S. Ganeshan, and S. Das Sarma, Quantum nonergodicity and fermion localization in a system with a single-particle mobility edge, Phys. Rev. B **93**, 184204 (2016).

[20] X. Li, X. P. Li, and S. Das Sarma, Mobility edges in one-dimensional bichromatic incommensurate potentials, Phys. Rev. B **96**, 085119 (2017).

[21] X. Li and S. Das Sarma, Mobility edge and interme-diate phase in one-dimensional incommensurate lattice potentials, Phys. Rev. B **101**, 064203 (2020).

[22] X. Deng, S. Ray, S. Sinha, G. V. Shlyapnikov, and L. Santos, One-Dimensional Quasicrystals With Power-Law Hopping, Phys. Rev. Lett. **123**, 025301 (2019).

[23] S. Das Sarma, S. He, and X. C. Xie, Mobility Edge In A Model One-Dimensional Potential, Phys. Rev. Lett. **61**, 2144 (1988).

[24] S. Das Sarma, S. He, and X. C. Xie, Localization, mobility edges, and metal-insulator transition in a class of one-dimensional slowly varying deterministic potentials, Phys. Rev. B **41**, 5544 (1990).

[25] Y. Wang, X. Xia, L. Zhang, H. Yao, S. Chen, J. You, Q. Zhou, and X. Liu, One Dimensional Quasiperiodic Mosaic Lattice With Exact Mobility Edges, Phys. Rev. Lett. **125**, 196604 (2020).

[26] D. Bernard and A. LeClair, *A Classification of Non-Hermitian Random Matrices* (Springer, Dordrecht, 2002), Vol. 73.

[27] K. Kawabata, K. Shiozaki, M. Ueda, and M. Sato, Symmetry And Topology In Non-Hermitian Physics, Phys. Rev. X **9**, 041015 (2019).

[28] H. Zhou and J. Y. Lee, Periodic table for topological bands with non-Hermitian symmetries, Phys. Rev. B **99**, 235112 (2019).

[29] C.-H. Liu and S. Chen, Topological classification of defects in non-Hermitian systems, Phys. Rev. B **100**, 144106 (2019).

[30] I. Y. Goldsheid and B. A. Khoruzhenko, Distribution Of Eigenvalues In Non-Hermitian Anderson Models, Phys. Rev. Lett. **80**, 2897 (1998).

[31] L. G. Molinari, Non-Hermitian spectra and Anderson localization, J. Phys. A: Math. Theor. **42**, 265204 (2009).

[32] H. Markum, R. Pullirsch, and T. Wettig, Non-Hermitian Random Matrix Theory And Lattice QCD With Chemical Potential, Phys. Rev. Lett. **83**, 484 (1999).

[33] J. T. Chalker and B. Mehlig, Eigenvector Statistics In Non-Hermitian Random Matrix Ensembles, Phys. Rev. Lett. **81**, 3367 (1998)

[34] N. Hatano and D. R. Nelson, Localization Transitions In Non-Hermitian Quantum Mechanics, Phys. Rev. Lett. **77**, 570 (1996).

[35] N. Hatano and D. R. Nelson, Vortex pinning and non-Hermitian quantum mechanics, Phys. Rev. B **56**, 8651 (1997).

[36] N. Hatano and D. R. Nelson, Non-hermitian delocalization and eigenfunctions, Phys. Rev. B **58**, 8384 (1998).

[37] A. V. Kolesnikov and K. B. Efetov, Localization- Delocalization Transition In Non-Hermitian Disordered Systems, Phys. Rev. Lett. **84**, 5600 (2000).

[38] Z. Gong, Y. Ashida, K. Kawabata, K. Takasan, S. Higashikawa, and M. Ueda, Topological Phases Of Non-Hermitian Systems, Phys. Rev. X **8**, 031079 (2018).

[39] D.-W. Zhang, L.-Z. Tang, L.-J. Lang, H. Yan, and S.-L. Zhu, Non-hermitian topological anderson insulators, Sci. China Phys. Mech. Astron. **63**, 267062 (2020).

[40] J. Claes and T. L. Hughes, Skin effect and winding number in disordered non-Hermitian systems, Phys. Rev. B **103**, L140201 (2021).

[41] L.-Z. Tang, L.-F. Zhang, G.-Q. Zhang, and D.-W. Zhang, Topological Anderson insulators in two-dimensional non-Hermitian disordered systems, Phys. Rev. A **101**, 063612 (2020).

[42] A. F. Tzortzakakis, K. G. Makris, and E. N. Economou, Non-hermitian disorder in two-dimensional optical lattices, Phys. Rev. B **101**, 014202 (2020).

[43] Y. Huang and B. I. Shklovskii, Anderson transition in three-dimensional systems with non-Hermitian disorder, Phys. Rev. B **101**, 014204 (2020).

[44] A. Jazaeri and I. I. Satija, Localization transition in incommensurate non-hermitian systems, Phys. Rev. E **63**, 036222 (2001).

[45] C. Yuce, $\mathcal{PT}$ symmetric Aubry-Andre model, Phys. Lett. A **378**, 2024 (2014).

[46] Q.-B. Zeng, S. Chen, and R. Lu, Anderson localization in the non-Hermitian Aubry-Andre-Harper model with physical gain and loss, Phys. Rev. A **95**, 062118 (2017).

[47] H. Jiang, L. J. Lang, C. Yang., S. L. Zhu, and S. Chen, Interplay of non-hermitian skin effects and anderson localization in nonreciprocal quasiperiodic lattices, Phys. Rev. B **100**, 054301 (2019).

[48] S. Longhi, Metal-insulator phase transition in a non-hermitian aubry-andré-harper model, Phys. Rev. B **100**, 125157 (2019).

[49] S. Longhi, Topological Phase Transition In Non-Hermitian Quasicrystals, Phys. Rev. Lett. **122**, 237601 (2019).

[50] Q. B. Zeng, Y. B. Yang, and Y. Xu, Topological phases in non-hermitian aubry-andré-harper models, Phys. Rev. B **101**, 020201(R) (2020).

[51] Y. Liu, X.-P. Jiang, J. Cao, and S. Chen, Non-Hermitian mobility edges in one-dimensional quasicrystals with parity-time symmetry, Phys. Rev. B **101**, 174205 (2020).

[52] Q.-B. Zeng and Y. Xu, Winding numbers and generalized mobility edges in non-Hermitian systems, Phys. Rev. Res. **2**, 033052 (2020).

[53] T. Liu, H. Guo, Y. Pu, and S. Longhi, Generalized Aubry-Andre self-duality and mobility edges in non-Hermitian quasiperiodic lattices, Phys. Rev. B **102**, 024205 (2020).

[54] Y. Liu, Y. Wang, X.-J. Liu, Q. Zhou, and S. Chen, Exact mobility edges, PT-symmetry breaking and skin effect in one-dimensional non-Hermitian quasicrystals, Phys. Rev. B **103**, 014203 (2021).

[55] X. Cai, Boundary-dependent self-dualities, winding numbers and asymmetrical localization in non-Hermitian quasicrystals, Phys. Rev. B **103**, 014201 (2021).

[56] Y. Liu, Q. Zhou, and S. Chen, Localization transition, spectrum structure and winding numbers for one-dimensional non-Hermitian quasicrystals, arXiv:2009.07605.

[57] S. Y. Jitomirskaya, Metal-insulator transition for the almost mathieu operator, Ann. Math. **3**, 150 (1999).

[58] A. Avila, The absolutely continuous spectrum of the almost Mathieu operator, arXiv:0810.2965.

[59] A. Avila, J. You, and Q. Zhou, Sharp phase transitions for the almost Mathieu operator, Duke. Math. J. **166**, 2697 (2017).

[60] A. Avila, Global theory of one-frequency Schröinger operators, Acta. Math. **215**, 1 (2015).

[61] Y. Wang, X. Xia, Y. Wang, Z. Zheng and X. j. Liu, arXiv: Duality between two generailized Aubry-Andre models with exact mobility edges, arXiv:2012.09756.

[62] X. Xia, Y. J. Wang, J. G. You, Z. H. Zheng, and Q. Zhou, Exact mobility edges for 1D quasicrystals (unpublished).

[63] C. M. Bender and S. Boettcher, Real Spectra In Non-Hermitian Hamiltonians Having PT Symmetry, Phys. Rev. Lett. **80**, 5243 (1998).

[64] S. Yao and Z. Wang, Edge States And Topological Invariants Of Non-Hermitian Systems, Phys. Rev. Lett. **121**, 086803 (2018).

[65] Y. Xiong, Why does bulk boundary correspondence fail in some non-Hermitian topological models, J. Phys. Commun. **2**, 035043 (2018).

[66] V. M. Martinez Alvarez, J. E. Barrios Vargas, and L. E. F. Foa Torres, Non-Hermitian robust edge states in one dimension: Anomalous localization and eigenspace condensation at exceptional points, Phys. Rev. B **97**, 121401(R) (2018).

[67] F. K. Kunst, E. Edvardsson, J. C. Budich, and E. J. Bergholtz, Biorthogonal, Bulk-Boundary Correspondence In Non-Hermitian Systems, Phys. Rev. Lett. **121**, 026808 (2018).

[68] C. H. Lee and R. Thomale, Anatomy of skin modes and topology in non-Hermitian systems, Phys. Rev. B **99**, 201103(R) (2019).

[69] If the non-Hermitian disorder or quasiperiodic systems are in the localzied phase, the systems are not sensitive to the boundary condition. For the type of Hatano-Nelson model under the open boundary condition, the imaginary vector potential h can be removed by making a similar transformation, and the system can be transformed to a Hermitian system. This gives a straightforward explanation why disordered states of the type of Hatano-Nelson model have real eigenvalues. On the other hand, if the systems are in the extended phase, their eigenvalues are sensitive to boundary conditions. Although the systems under the open boundary condition still have real eigenvalues even in the extended phase, they have complex eigenvalues under the periodic boundary condition.

[70] M. A. Bandres, M. C. Rechtsman, and M. Segev, Topological Photonic Quasicrystals: Fractal Topological Spectrum And Protected Transport, Phys. Rev. X **6**, 011016 (2016).

[71] A. Regensburger, C. Bersch, B. Hinrichs, G. Onishchukov, A. Schreiber, C. Silberhorn, and U. Peschel, Photon Propagation In A Discrete Fiber Network: An Interplay Of Coherence And Losses, Phys. Rev. Lett. **107**, 233902 (2011).

[72] A. Regensburger, C. Bersch, M. A. Miri, G. Onishchukov, D. N. Christodoulides, and U. Peschel, Parity-time synthetic photonic lattices, Nature (London) **488**, 167 (2012).

[73] M. Wimmer, M. A. Miri, D. Christodoulides, and U. Peschel, Observation of Bloch oscillations in complex PT-symmetric photonic lattices, Sci. Rep. **5**, 17760 (2015).

[74] I. D. Vatnik, A. Tikan, G. Onishchukov, D. V. Churkin, and A. A. Sukhorukov, Anderson localization in synthetic photonic lattices, Sci. Rep. **7**, 4301 (2017).

[75] S. Derevyanko, Disorder-aided pulse stabilization in dissipative synthetic photonic lattices, Sci. Rep. **9**, 12883 (2019).

[76] S. Weidemann, M. Kremer, T. Helbig, T. Hofmann, A. Stegmaier, M. Greiter, R. Thomale, and A. Szameit, Topological funneling of light, Science **368**, 311 (2020).